

## Local structure and NO adsorption/desorption property of Pd<sup>2+</sup> cations at different paired Al sites in CHA zeolite

Shunsaku Yasumura<sup>a</sup>, Taihei Ueda<sup>a</sup>, Hajime Ide<sup>a</sup>, Katsumasa Otsubo<sup>b</sup>, Chong  
Liu<sup>c</sup>, Nao Tsunoji<sup>b</sup>, Takashi Toyao<sup>a,d</sup>, Zen Maeno<sup>a\*</sup>, Ken-ichi Shimizu<sup>a,d\*</sup>

<sup>a</sup> Institute for Catalysis, Hokkaido University, N-21, W-10, Sapporo 001-0021,  
Japan

<sup>b</sup> Graduate School of Advanced Science and Engineering, Hiroshima University,  
Higashi-Hiroshima 739-8527, Japan

<sup>c</sup> State Key Laboratory of Structural Chemistry, Fujian Institute of Research on  
the Structure of Matter, Chinese Academy of Sciences, Fuzhou, Fujian 350002,  
China

<sup>d</sup> Elements Strategy Initiative for Catalysts and Batteries, Kyoto University,  
Katsura, Kyoto 615-8520, Japan

\*Corresponding author

Zen Maeno

E-mail: [maeno@cat.hokudai.ac.jp](mailto:maeno@cat.hokudai.ac.jp)

Ken-ichi Shimizu

E-mail: [kshimizu@cat.hokudai.ac.jp](mailto:kshimizu@cat.hokudai.ac.jp)

## DFT Calculations

Spin-polarized DFT calculations were performed by means of the periodic boundary condition under the Kohn–Sham formulation<sup>1,2</sup> with the Vienna ab-initio simulation package (VASP)<sup>3,4</sup>. The generalized gradient approximated Perdew-Burke-Ernzerhof (GGA-PBE) functional<sup>5</sup> was applied as electron exchange-correlation. The projected augmented waves (PAW) method was utilized for the Kohn-Sham equations<sup>6,7</sup>. All atoms were allowed to fully relax during all calculations along with the D3(BJ)vdw correction<sup>8,9</sup>. A cut-off energy of the plane basis set was set to 500 eV. The  $\Gamma$  point was used for Brillouin zone sampling.<sup>10</sup> The lattice constants of unit cell were fixed as given in the International Zeolite Association (IZA) database ( $a = b = 13.675 \text{ \AA}$ ,  $c = 14.767 \text{ \AA}$ ,  $\alpha = \beta = 90.0^\circ$  and  $\gamma = 120^\circ$ ) during the calculations<sup>11</sup>.

The relative formation energy of Pd cation ( $\Delta E_f$ ) is defined as

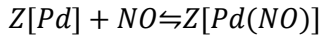
$$\Delta E_f = E_{Pd/CHA} - E_{CHA_{2H}} - \frac{1}{2}E_{PdO_{bulk}} + E_{H_2O}$$

where  $E_{Pd/CHA}$ ,  $E_{CHA_{2H}}$ ,  $E_{PdO_{bulk}}$ , and  $E_{H_2O}$  are the total energy of the unit cell of CHA zeolite containing one Pd cation at considered Al sites, that of the zeolite containing two protons for charge compensation, the energy of the bulk PdO (two Pd and O atoms are included in the unit cell), and the energy of isolated H<sub>2</sub>O molecule within the same unit cell as CHA zeolite, respectively. The adsorption energy of NO on Pd<sup>2+</sup> cation is defined as follows.

$$E_{ad} = E_{NO-Pd/CHA} - E_{Pd/CHA} - E_{NO}$$

In this way,  $E_{NO-Pd/CHA}$  is the total energy of considered CHA zeolite model containing one NO molecule adsorbed on one Pd<sup>2+</sup> cation.  $E_{NO}$  represents the total energies of a unit cell of gaseous NO within a large cubic cell ( $a = b = c = 10 \text{ \AA}$ ).

Ab initio thermodynamic analysis was performed to consider the effect of partial pressure of NO as well as temperature on NO adsorbed on Pd<sup>2+</sup> cation in CHA zeolites. Enthalpies and entropies at each temperature and at the standard state pressure (0.1 MPa) were obtained from NIST thermodynamic table to utilize this analysis.<sup>12</sup> The following equilibrium reaction was considered for figuring the phase diagrams;



where the reaction energy is denoted as

$$\Delta E = E_{Z[PdNO]} - E_{Z[Pd]} - E_{NO}$$

The Gibbs free energy ( $\Delta G$ ) is described as

$$\Delta G(T,p) = [\Delta E - \Delta\mu_{NO}]$$

The change of the chemical potential of NO as a function of  $T$  and pressure of NO ( $p_{NO}$ ) is defined as

$$\Delta\mu_{NO}(T,p) = [\Delta\mu_{0\ NO}(T) + RT\ln\left(\frac{p_{NO}}{p_0}\right)]$$

To discuss the molecular–orbital interactions, DFT calculations were employed with the Gaussian 16 package using a cluster model. The cluster model was obtained from the optimized structure models within a periodic boundary condition and geometry optimization were performed for every model with fixing terminating H atoms. The hybrid  $\omega$ B97X-D functional, which was well applied for the evaluation of relative energy of zeolite<sup>13–15</sup>, was used with the 6-31G\*\* basis sets and SDD basis sets for Si, Al, O, and H atoms and Pd atom, respectively.<sup>16,17</sup> Charge decomposition analysis (CDA) was performed by using Multiwfn program.<sup>18</sup>

### **NO adsorption experiments using FTIR spectroscopy**

The NO adsorption on Pd-CHA was monitored by infrared (IR) spectroscopy. The IR spectra were recorded on a JASCO FT/IR-4600 spectrometer by using a home-made *in-situ* cell equipped with  $\text{CaF}_2$  windows. 20 scans were accumulated for each spectrum and a triglycine sulfate (TGS) detector was applied. Pd-exchanged CHA (Pd-CHA) was prepared through the impregnation as follows. First, 1.0 g of CHA zeolite (Tosoh,  $\text{NH}_4^+$ -type,  $\text{SiO}_2/\text{Al}_2\text{O}_3 = 13.7$ ,  $\text{NH}_4$ -CHA) were suspended in an aqueous solution containing 0.101, 0.202, 0.409, 0.619, 0.834, and 1.142 g of  $\text{Pd}(\text{NO}_3)_2$  (Kojima Chemicals Co., Ind.), giving Pd-modified CHA with the loading amounts of 0.5, 1, 2, 3, 4, and 5.4 wt%, respectively. The water was evaporated from the mixture, and the mixture was dried in an oven and calcined at 600 °C in air for 1 h. 50mg of self-supported disks (20 mm diameter) of the prepared Pd-modified CHA zeolite were set in *in-situ* IR cell (Figure S1), and first calcined under a flow of 10 %  $\text{O}_2/\text{He}$  (100 mL/min) for 30 min at 600 °C, followed by subjecting to a flow of 0.5%  $\text{H}_2$  (100 mL/min) for 30 min at 500 °C. After purging with He for 10 min, the disks were further subjected to a flow of 4% NO (10 mL/min) for 2 h at 600 °C to achieve solid-state ion-exchange.<sup>19</sup> Then, background spectra were obtained under He flow at same temperatures as the measuring ones before the NO adsorption measurement. After taking the background spectrum, the NO adsorption measurement was started and then 0.1% NO/He flowed (100 mL/min). The IR spectra were collected after the intensity of band derived from NO on  $\text{Pd}^{2+}$  cation (NO- $\text{Pd}^{2+}$ ) around 1860  $\text{cm}^{-1}$  reached its equilibrium at each measuring temperatures.

## NO-TPD measurement

Temperature programmed desorption measurement under NO flow (NO-TPD) was performed using a fixed continuous flow system. An 80 mg of sample was put into a quartz reactor with quartz wool as a bed. After NO-facilitated solid-state ion-exchange reaction was done as explained above, the temperature of the reactor was set to 350 °C at which NO<sup>+</sup> species at a zeolite anion was scarcely observed by *in-situ* IR measurement.<sup>20</sup> The outlet gas from the reactor was directly connected to a home-made IR gas cell to monitor the NO concentration by IR measurement. In the first 400s of data recording, a flow of 0.1% NO/He was passing through the bypass line, and then the feed was switched to the heated reactor at 350 °C. At 1000s, the temperature of the reactor started to ramp up in 20 °C/min to 750 °C, and then the reactor temperature was maintained.

The adsorption energy of the observed NO desorption peaks was evaluated by using Redhead analysis.<sup>21</sup> For first order desorption, the activation energy is evaluated from the peak position by using

$$\frac{Ea}{RT_p} = \ln \left( \frac{\nu T_p}{\beta} \right) - 3.64$$

where  $Ea$ ,  $R$ ,  $T_p$ ,  $\nu$ , and  $\beta$  are the activation energy, gas constant, the temperature of desorption peak top, the desorption prefactor, and ramping rate. The applied value of  $\nu$  ( $3.81 \times 10^{-8}$ ) was obtained by the liner plot of following equation.

$$\ln \left( \frac{T_p^2}{\beta} \right) = \frac{Ea}{RT_p} + \ln \left( \frac{E_a}{R\nu} \right)$$

### **CHA zeolites with different amount of paired Al sites in 6MR**

Three type of CHA zeolites with different amount of paired Al sites were synthesized by changing the ratio of inorganic and organic structure-directing agents ( $\text{Na}^+$  cation (as NaOH) and *N,N,N*-trimethyl-1-adamantylammonium cation ( $\text{TMAda}^+$ ) as TMAdaOH) according to the previous reports with slight modification.<sup>22</sup> TMAdaOH (Sachem), NaOH (Merck), distilled water, aluminum hydroxide (dry gel, Stream Chemical), and colloidal silica (Ludox HS-40, Aldrich) were mixed to obtain a synthesis gel with a composition of 1:0.05:0.5~0.3:0~0.2:44 of Si/Al/TMAdaOH/NaOH/ $\text{H}_2\text{O}$ . The resultant gel was transferred to a 100 cm<sup>3</sup> Teflon-lined stainless steel autoclave (stirring-type hydrothermal synthesis reactor, R-100, Hiro Company, Japan) and heated to 160 °C for 6 days at 30 rpm. The obtained solid product was separated by centrifugation and washed thoroughly with deionized water until the pH of the supernatant was close to neutral. The solid was dried overnight at 70 °C yielding the as-synthesized sample. To remove the organics in the sample, the as-made zeolites were calcined in air at 580 °C for 10 h (heating rate of 1 °C min<sup>-1</sup>). The  $\text{Na}^+$  cations in the obtained CHA zeolites were removed by ion-exchange using an aqueous solution containing  $\text{NH}_4\text{NO}_3$  (ca. 1.0 mol/L) for 24 h at ambient conditions.  $\text{NH}_4^+$ -type CHA zeolites were used for the preparation of Pd-CHA to investigate the effect of Al distributions. The amount of paired Al site was estimated by aqueous-phase ion-exchange reaction with  $\text{Co}^{2+}$  cations according to the same paper. The synthesized  $\text{NH}_4^+$ -type CHA zeolites were converted to their  $\text{H}^+$  form by calcination under air flow at 500 °C for 4 h and then suspended in a 0.25 mol/L aqueous solution of  $\text{Co}(\text{NO}_3)_2 \cdot 6\text{H}_2\text{O}$  (98%, Wako Pure Chemical Industries, Ltd.). These mixtures were stirred at room temperature for 4 hours and separated by centrifugation, followed by washing with deionized water. This centrifugation-washing procedure was repeated

three times. The resulting solids were dried 90 °C in the air and then calcined at 500 °C under air flow for 4 h to afford Co-exchanged CHA zeolites. The Si/Al ratio and the amount of loaded Co<sup>2+</sup> cations were quantified by inductively coupled plasma-atomic emission spectroscopy (ICP-AES) measurements (Seiko SPS7000 and ICPE-9000), independently. The synthesis conditions and characterization results are summarized in Table S1.

Tables and Figures

**Table S1** Synthesis conditions and characterizations of CHA zeolites with different amount of paired Al sites in 6MR.

Sample	NaOH/SiO <sub>2</sub>	TMAdaOH/SiO <sub>2</sub>	Si/Al <sup>a</sup>	Loaded Co cation <sup>a</sup>	Al <sub>6MR pair</sub> /Al <sup>b</sup>
CHA(0.7)	-	0.50	12.0	4.2 μmol/g	0.7%
CHA(2.2)	0.10	0.40	15.4	11.2 μmol/g	2.2%
CHA(7.1)	0.20	0.30	16.5	34.1 μmol/g	7.1%

Synthesis conditions: Si/Al = 20, H<sub>2</sub>O/SiO<sub>2</sub> = 44, Temp. 160 °C, Time = 6 days, Rotation speed = 30 rpm. <sup>a</sup> Determined by ICP-AES. <sup>b</sup> Estimated from Si/Al values and amounts of loaded Co cations.

**Table S2** The amount of NO adsorption/desorption determined by the NO adsorption and the following TPD measurement (Fig. 7).

	NO adsorption (mmol/g)	NO desorption (mmol/g)
2 wt% Pd-CHA	0.034	0.018
3 wt% Pd-CHA	0.069	0.050
4 wt% Pd-CHA	0.111	0.085
5.4 wt% Pd-CHA	0.171	0.130

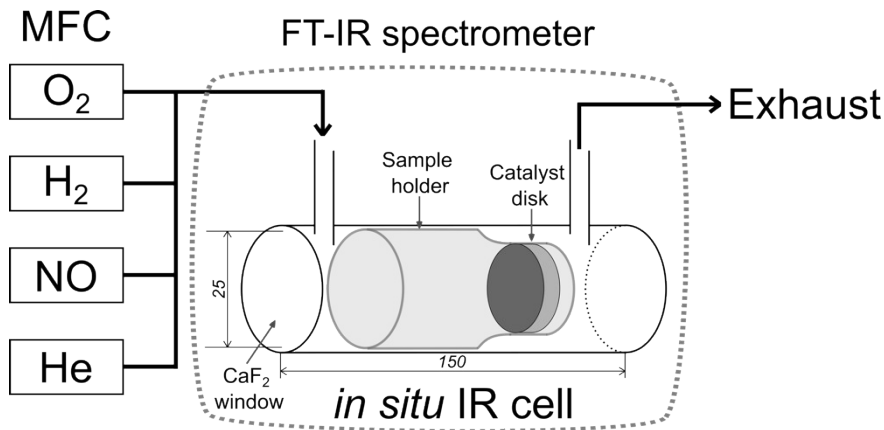


**Fig. S1.** Schematic view of the used setup for *in-situ* IR measurement. Inner diameter and length of the cell are provided with a unit of mm.



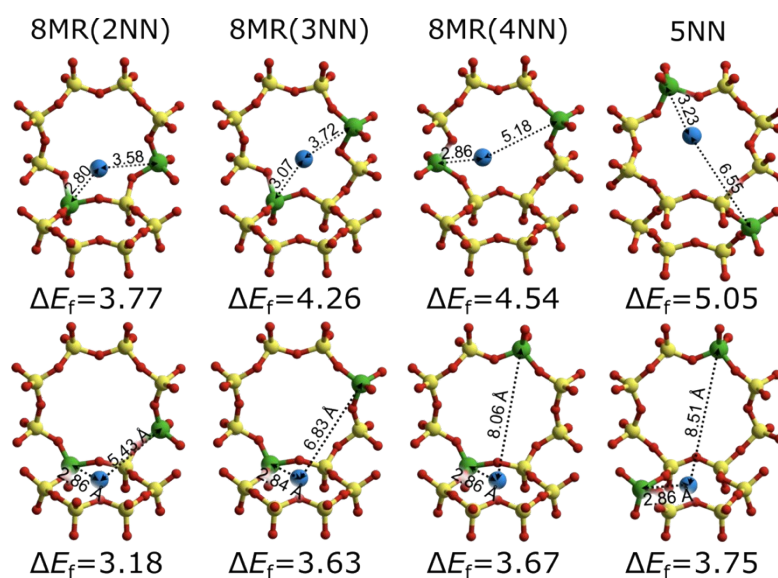


**Fig. S2** The optimized structure of considered models with relative formation energies ( $\Delta E_f$ , the definition is described in the experiential section). Yellow: Si, Red: O, Green: Al, Blue: N, Cyan: Pd. Only atoms around Pd are shown for clarity.

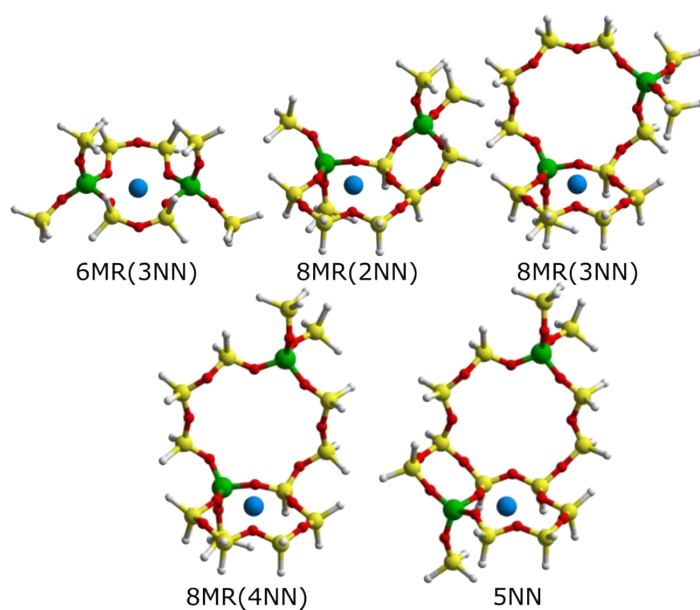


**Fig. S3** The cluster models used for the molecular orbital analysis. Yellow: Si, Red: O, Green: Al, Blue: N, Cyan: Pd, White: H.

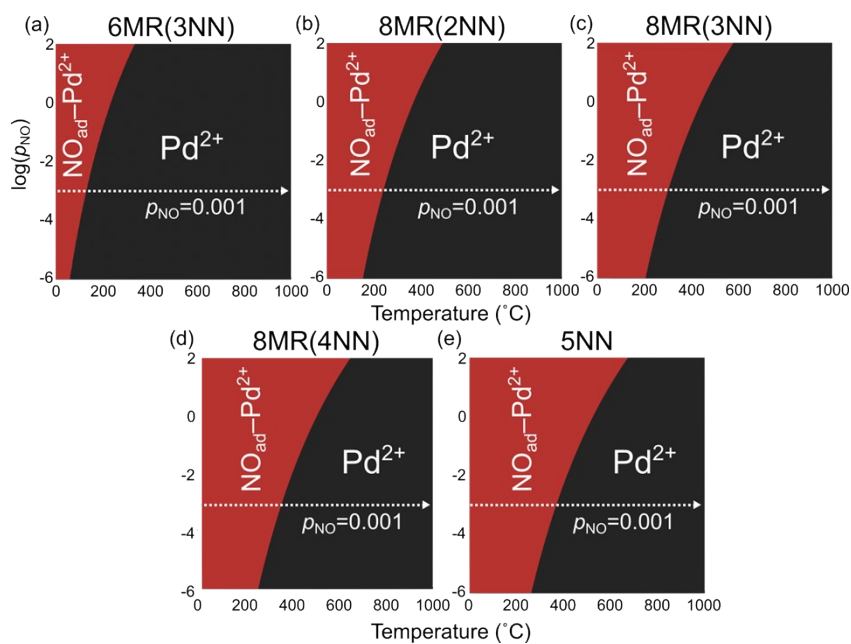
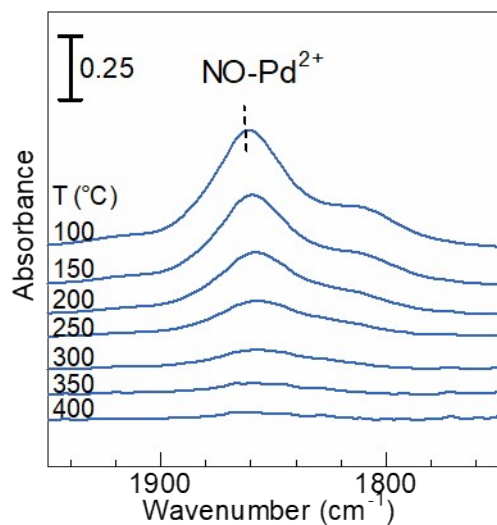
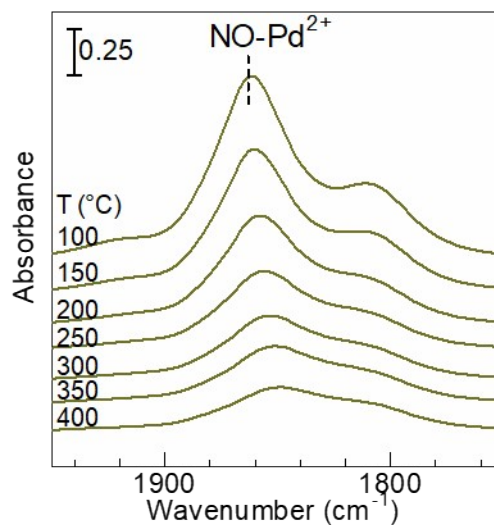


**Fig. S4** Thermodynamic phase diagrams for bare  $\text{Pd}^{2+}$  cation ( $\text{Pd}^{2+}$ ) and NO adsorbed one ( $\text{Pd}^{2+}-\text{NO}_{\text{ad}}$ ) at each paired Al site as a function of temperature and partial pressure of NO

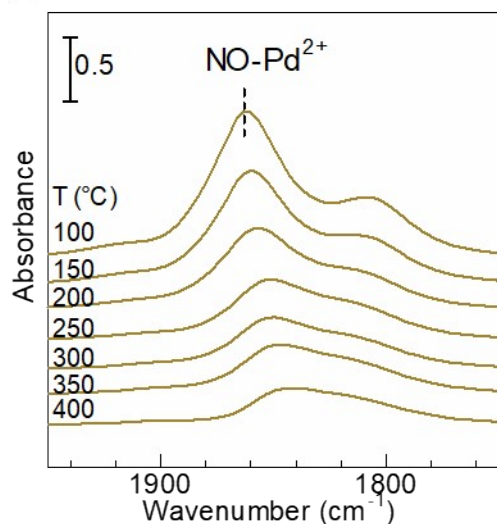
(a) 1 wt% Pd-CHA



(b) 2 wt% Pd-CHA



(c) 3 wt% Pd-CHA



(d) 4 wt% Pd-CHA

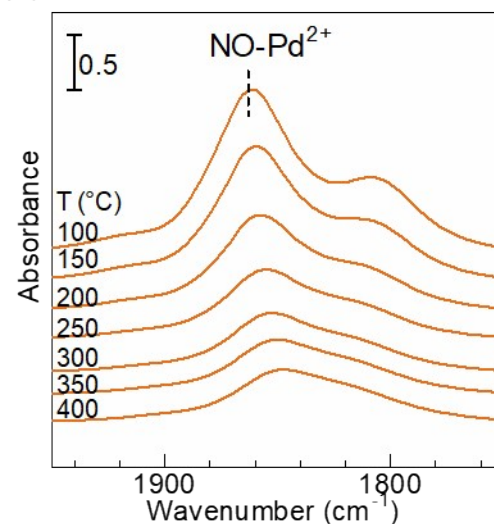


**Fig. S5** *In-situ* IR spectra of NO-Pd<sup>2+</sup> species over (a) 1 wt%, (b) 2 wt%, (c) 3 wt%, and (d) 4 wt% Pd-CHA under a flow of 0.1% NO (total flow: 100 ml/min). The background spectra were taken under He flow at each measuring temperature before subjecting to NO.

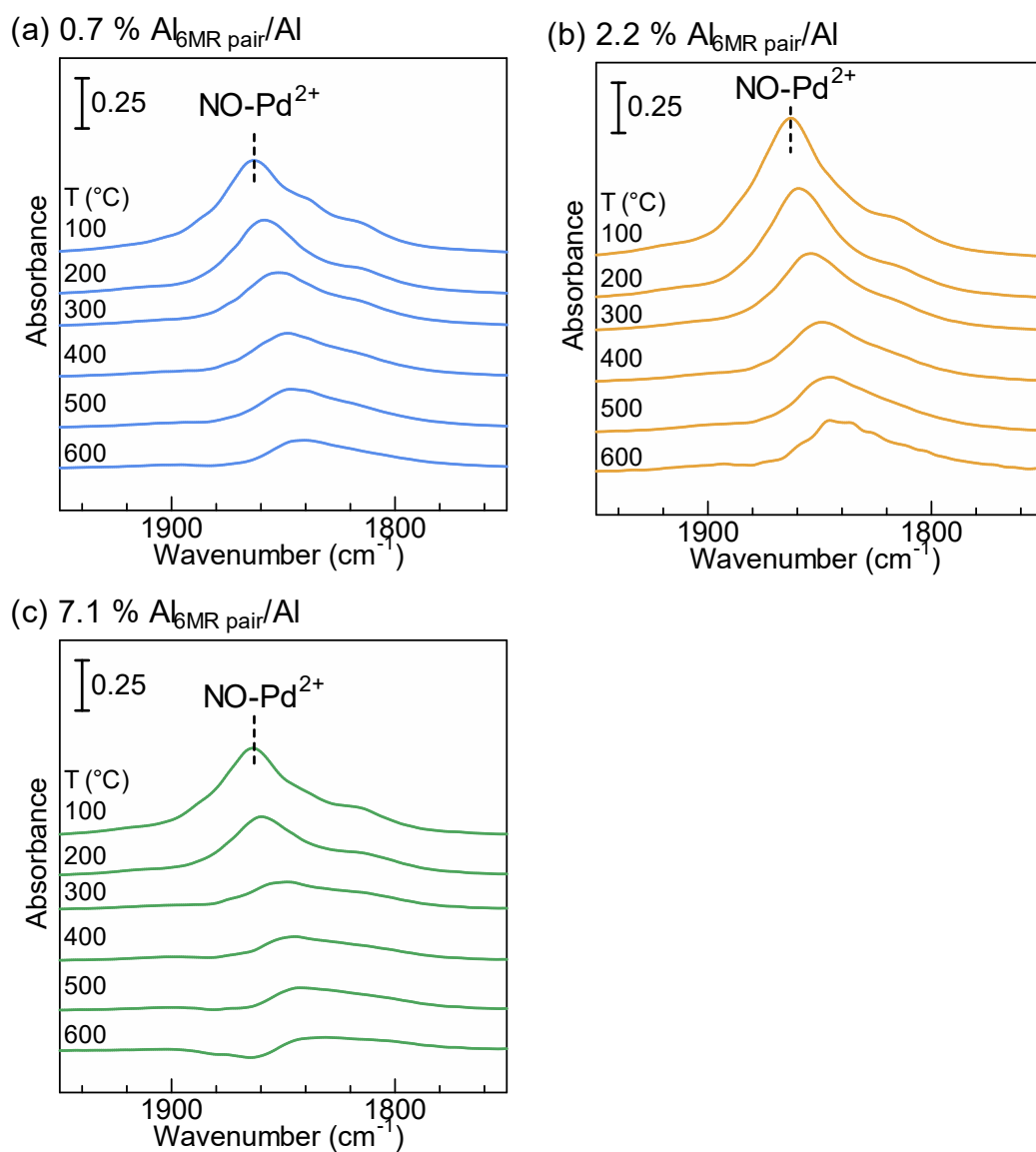


**Fig. S6** *In-situ* IR spectra of NO-Pd<sup>2+</sup> species over prepared 1 wt% Pd-CHA with different ratios of 6MR paired Al sites ( $\text{Al}_{6\text{MR pair}}/\text{Al}$ ) (a) 0.7%, (b) 2.2%, and (c) 7.1%) under a flow of 0.1% NO (total flow: 100 ml/min). The background spectra were taken under He flow at each measuring temperature before subjecting to NO.

## References

- 1 P. Hohenberg and W. Kohn, *Phys. Rev. B*, 1964, **136**, B864–B871.
- 2 W. Kohn and L. J. Sham, *Phys. Rev. A*, 1965, **140**, A1133–A1138.
- 3 G. Kresse and J. Furthmüller, *Phys. Rev. B*, 1996, **54**, 11169–11186.
- 4 G. Kresse and J. Furthmüller, *Comput. Mater. Sci.*, 1996, **6**, 15–50.
- 5 J. P. Perdew, K. Burke and M. Ernzerhof, *Phys. Rev. Lett.*, 1996, **77**, 3865–3868.
- 6 P. E. Blöchl, *Phys. Rev. B*, 1994, **50**, 17953–17979.
- 7 D. Kresse, G.; Joubert, G. Kresse and D. Joubert, *Phys. Rev. B*, 1999, **59**, 1758–1775.
- 8 S. Grimme, J. Antony, S. Ehrlich and H. Krieg, *J. Chem. Phys.*, 2010, **132**, 154104.
- 9 S. Grimme, S. Ehrlich and L. Goerigk, *J. Comput. Chem.*, 2011, **32**, 1456–1465.
- 10 H. J. Monkhorst and J. D. Pack, *Phys. Rev. B*, 1976, **13**, 5188–5192.
- 11 C. Baerlocher and L. B. McCusker, Database of Zeolite Structures, <http://www.iza-structure.org/databases>, (accessed 10 June 2019).
- 12 M. W. Chase, J. C.A. Davies, J. J.R. Downey, D. J. Frurip, R. A.

- McDonald and A. N. Syverud, *NIST-JANAF Thermochemical Tables*, the U.S. Department of Commerce, Washington, DC, 2nd edn., 1985.
- 13 J. Da Chai and M. Head-Gordon, *Phys. Chem. Chem. Phys.*, 2008, **10**, 6615–6620.
- 14 N. Mardirossian and M. Head-Gordon, *Mol. Phys.*, 2017, **115**, 2315–2372.
- 15 E. Mansoor, M. Head-Gordon and A. T. Bell, *ACS Catal.*, 2018, **8**, 6146–6162.
- 16 F. Weigend and R. Ahlrichs, *Phys. Chem. Chem. Phys.*, 2005, **7**, 3297–3305.
- 17 F. Weigend, *Phys. Chem. Chem. Phys.*, 2006, **8**, 1057–1065.
- 18 T. Lu and F. Chen, *J. Comput. Chem.*, 2012, **33**, 580–592.
- 19 S. Yasumura, H. Ide, T. Ueda, Y. Jing, C. Liu, K. Kon, T. Toyao, Z. Maeno and K. Shimizu, *JACS Au*, 2021, **1**, 201–211.
- 20 S. Yasumura, C. Liu, T. Toyao, Z. Maeno and K. Shimizu, *J. Phys. Chem. C*, 2021, **125**, 1913–1922.
- 21 P. A. Redhead, *Vacuum*, 1962, **12**, 274.
- 22 J. R. Di Iorio and R. Gounder, *Chem. Mater.*, 2016, **28**, 2236–2247.